Journal of Sound and Vibration (2001) **241**(2), 297–314
doi:10.1006/jsvi.2000.3269, available online at http://www.idealibrary.com on IDEAL®

SENSOR/ACTUATOR EQUATIONS FOR CURVED PIEZOELECTRIC FIBERS AND VIBRATION CONTROL OF COMPOSITE BEAMS USING FIBER MODAL ACTUATORS/SENSORS

D. C. SUN[†] AND L. TONG

Department of Aeronautical Engineering, The University of Sydney, NSW 2006, *Australia.*
E-mail: *Ltong@aero.esyd.edu.au*

(*Received* 28 *January* 2000, *and in final form* 16 *August* 2000)

Vibration control of the composite beam integrated with curved piezoelectric fibers is investigated. Sensory and actuating equations of the curved piezoelectric fibers embedded in a composite slender beam are derived, and expressed in terms of line integrals. In addition, a new method for designing fiber modal sensors and modal actuators is presented by means of modulating the shapes of the curved piezoelectric fibers. The curvature shape of each modal sensor/actuator fiber can be determined by solving a differential equation. For a slender beam, an approximate solution is given. Based on the modal sensor fibers and modal actuator fibers, the modal control of the composite beam is performed independently. Finally, an illustrated example is given in which the effects of the curvatures of the fibers on the sensing signals are discussed.

1. INTRODUCTION

Piezoelectric materials have been increasingly used as the distributed sensors an actuators in vibration control and shape control of smart structures in the past decade. As a laminate, each piezoelectric layer is usually bonded on or embedded in the laminated continua such as beams, plates and shells [1–7]. Since the traditional discrete sensor and actuator are replaced by the distributed sensor and actuator, more accurate sensing and actuating can be realized, and consequently precise active control can be performed. Recent literature reviews [8–11] show that many theoretical, experimental and computational studies have been carried out on the piezoelectric smart structures, and significant achievements have been made on modelling, distributed sensing, distributed actuating, active control of the piezoelectric smart structures [12–18].

Besides the piezoelectric lamina and patches, the piezoelectric fibers are also used in the piezoelectric composites for vibration and acoustic control of the flexible structures. Active piezoelectric damping composite (APDC), as one of the piezoelectric fiber composites (PFC), has been used in hybrid vibration and acoustic control of structures. In such a piezoelectric fiber composite, the piezoelectric fibers are embedded across the thickness of the matrix, and the fibers are polarized along their length direction. Due to the high-damping property of the selected matrix, the APDC can be used as a component

[†]On leave from School of Mechanical Engineering, Hebei University of Technology, Tianjin 300130, People's Republic of China

0022-460X/01/120297 + 18 $35.00/0

for vibration and acoustic control of flexible structures both actively and passively [19, 20].

Another kind of piezoelectric fiber composite has been developed aimed at enhancing the performance of the actuator composites. In this composite material, the piezoelectric fibers are aligned in the plane of the plate-like composite and they can be polarized either across their thickness direction or along their length direction [21–23]. Like the piezoelectric laminates, the PFC actuators can also be used as a ply integrated into the structures, which may provide some particular actuating functions that the monolithic piezoelectric ply cannot give.

In recent years, the PFC has attracted a wide range of attention and a great effort has been devoted to the development of micro-mechanical models, finite element model and manufacturing technologies of the piezoelectric composite because of the advantages of the piezoelectric fiber composite over the piezoelectric material itself. Firstly, the combination of the piezoelectric fibers and other kinds of strong fibers as well as the soft matrix will increase the composite robustness to damage compared with the brittle monolithic piezoelectric ceramics itself. The PFC sensor and actuator can even be made flexible enough to fit on the special surfaces of the structures. Secondly, some PFC sensors and actuators with particular functions, such as APDC mentioned above, may be obtained by combining the piezoelectric fibers and some functional matrix materials. Thirdly, some special needs in some fields such as vibration control, damage detection and health monitoring may be met by the PFC sensors and actuators by delicately shaping the piezoelectric fibers in the composite.

In the previous studies, the straight piezoelectric fibers are usually used in the composite. However, in some circumstances, the curved piezoelectric fibers may add more dimensions to design sensors and actuators. For instance, the curved fibers are permitted to design into special shape in accordance with some particular purposes such as damage detection and modal sensors. Therefore, it is necessary to derive the sensor equations and actuator equations of the curved piezoelectric fibers for a better understanding of the effects of the curvatures of the piezo-fibers on the sensing and actuating functions.

The modal sensors and modal actuators can be implemented by the distributed piezoelectric laminates and the independent modal space control [24] can be performed without any observation and control spillover [25–29]. One method of designing modal sensor/actuator is to shape the electrodes patterns together with varying the polling directions of the piezoelectric layers. Another method to design the modal sensor/actuator is presented based on the concessive segmentation of the piezoelectric layers to overcome the drawback of the previous method [30, 31]. In addition, to perform the vibration control of large flexible structures, quasi-modal sensors and modal actuators are introduced by using discretely distributed piezoelectric wafers by means of optimal placement of the wafers, spillover analysis as well as digital filter [32]. With the modal sensors and modal actuators, effective control of the flexible structures has been demonstrated in many investigations. However, all these methods may not be used directly to design the fiber modal sensor/actuator since the piezoelectric fibers are usually very thin. Thus, the main effort of this paper is devoted to design the fine fiber modal sensor/actuator by fully taking advantage of the characteristics of the curved piezoelectric fibers.

In this paper, the modelling and vibration control of a composite beam with curved piezoelectric fibers in planes perpendicular to its neutral plane is investigated. The sensory and actuating equations of the curved piezoelectric fibers are derived. A method for designing modal sensor and modal actuator is presented by modulating the shapes of the piezoelectric fibers. Based on the modal sensors and modal actuators, independent modal

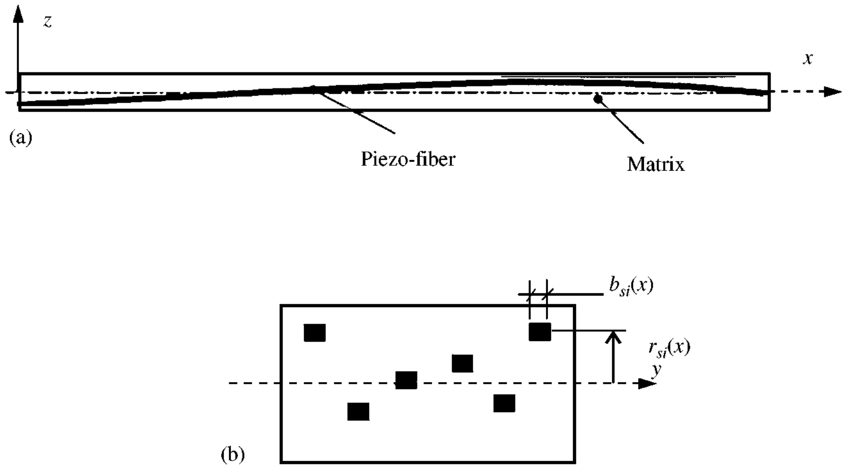

Figure 1. The composite beam with curved piezoelectric fibers: (a) curved piezofiber in the matrix; (b) cross-section (not on scale).

space control is realized for vibration control of the composite beam. A simulation example is given to demonstrate the presented method.

2. BASIC EQUATIONS

Consider a slender composite beam in which several curved piezoelectric fibers with their own electrodes are embedded as sensors and actuators. The cross-section of each piezoelectric fiber is assumed to be rectangular, and its polling direction is along its thickness direction. The upper or lower electrode of each curved piezoelectric fiber is no longer in a plane, and the middle line of each fiber is in a plane perpendicular to the mid-plane of the composite beam, as shown in Figure 1.

There are no manufacturing technologies available as yet. However, there are two possible methods of embedding the curved (shaped) piezoelectric fibers into the host beam. In the first method, the host beam is sliced into a number of slender sub-beams across the width direction, then the curved fibers may be sandwiched amongst those slender sub-beams via adhesive bonding, which in turn form the entire beam with embedded curved fibers. In the second method, the two surfaces in the width direction may be slotted, and the curved fibers may then be embedded in via bonding. In the second method, however, only two curved fibers can be attached to the host beam, while a number of fibers may be embedded into the host beam using the first method.

Assume that the piezoelectric fibers and the non-conductive matrix are bonded perfectly, and that the curvatures of the fibers are not very large due to the small thickness and length ratio of the beam. In the following derivation, only the transverse displacement of the composite beam is considered.

2.1. SENSOR EQUATIONS

The general constitutive equation of the piezoelectric sensors in C_{4v} or C_{6v} group has the following form:

$$D_3 = d_{31}\sigma_1 + d_{31}\sigma_2 + d_{33}\sigma_3 + d_{15}\tau_{23} + d_{15}\tau_{13}, \tag{1}$$

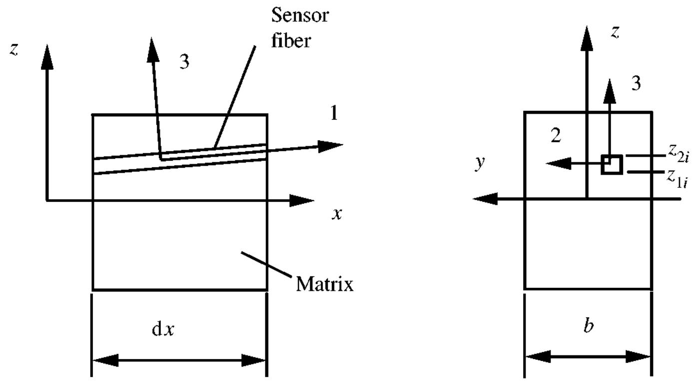

Figure 2. The stretch diagram on an element of the composite beam with sensor fiber.

where D_3 is the electric displacement in the polling direction (3-axis, as shown in Figure 2), d_{31} and d_{33} are the piezoelectric strain constants in the three orthogonal directions, and σ_1, σ_2 and σ_3 are the stresses in three directions respectively.

Using the co-ordinate transformation, the stresses of the sensor fiber can be obtained:

$$\sigma_1 = \sigma\cos^2\alpha, \qquad \sigma_2 = 0, \qquad \sigma_3 = \sigma\sin^2\alpha, \qquad \tau_{23} = \tau_{13} = 0, \tag{2}$$

where α is the angle between the tangent of the sensor fiber and the x-axis of the composite beam, and σ is the stress of the composite beam, which is given by

$$\sigma = Y_s\left(-z\frac{\partial^2 w}{\partial x^2}\right), \tag{3}$$

where z is the co-ordinate from the neutral plane of the composite beam, Y_s is Young's modulus of the piezoelectric sensor, and w is the transverse displacement of the composite beam.

The total electric charge of the ith sensor fiber can be evaluated by

$$q_i(t) = \int_{\Gamma_{si}} b_{si}\tfrac{1}{2}(D_{3i}(z_{1i}) + D_{3i}(z_{2i}))\,\mathrm{d}s, \quad i = 1, 2, \ldots, N_s, \tag{4}$$

where b_{si} is the width of the ith sensor fiber, Γ_{si} is the path occupied by the sensor fiber, and N_s is the number of the sensor fibers. Substituting equations (1)–(3) into equation (4), yields

$$q_i(t) = -\int_{\Gamma_{si}} b_{si}r_{si}(x)\frac{\partial^2 w}{\partial x^2}(e_{31i}\cos^2\alpha + e_{33i}\sin^2\alpha)\,\mathrm{d}s, \tag{5}$$

where e_{31i} and e_{33i} are the piezoelectric stress constants of the ith sensor fiber, and

$$r_{si}(x) = \frac{z_{1i} + z_{2i}}{2} \tag{6}$$

is the z co-ordinate of the mid-plane of the ith sensor fiber and called the shape function since it can completely determine the shape of the fiber for a piezoelectric sensor fiber with uniform width and thickness.

Assume that the path Γ_{si} in xz plane projected by the mid-plane of the ith sensor fiber, $z(x) = r_{si}(x)$ $(0 \leqslant x \leqslant l)$, is smooth, we have

$$\cos\alpha = \frac{1}{\sqrt{1 + r_{si}'^2}}, \qquad \sin\alpha = \frac{r_{si}'}{\sqrt{1 + r_{si}'^2}}, \qquad \mathrm{d}s = \mathrm{d}x\sqrt{1 + r_{si}'^2}, \tag{7}$$

where the superscript $'$ represents the first derivative with respect to x. Substituting equation (7) into equation (5), gives

$$q_i(t) = -\int_0^l b_{si} r_{si}(x) \frac{\partial^2 w}{\partial x^2} \left[e_{31i} + e_{33i} r_{si}'^2(x)\right] \frac{1}{\sqrt{1 + r_{si}'^2}} \mathrm{d}x, \tag{8}$$

where l is the length of the composite beam.

Differentiating equation (8) with respect to time t, the output currents of the ith sensor can be obtained as follows:

$$I_i(t) = \frac{\mathrm{d}q_i(t)}{\mathrm{d}t} = -\int_0^l b_{si} r_{si}(x) \frac{\partial^3 w}{\partial x^2\,\partial t} \left[e_{31i} + e_{33i} r_{si}'^2(x)\right] \frac{1}{\sqrt{1 + r_{si}'^2}} \mathrm{d}x. \tag{9}$$

Equations (8) and (9) are the sensor equations of the composite beam which establish the relationship between the fiber outputs and beam's transverse vibration. It should be noted that the output charge of each curved piezo-fiber sensor fiber is affected by its curvature.

When the curvature is very small so that $r_{si}'^2(x)$ can be neglected, the sensor equations (8) and (9) can be approximately simplified to the following form:

$$q_i(t) = -\int_0^l b_{si} e_{31i} r_{si}(x) \frac{\partial^2 w}{\partial x^2} \mathrm{d}x, \quad i = 1, 2, \ldots, N_s, \tag{10a}$$

$$I_i(t) = -\int_0^l b_{si} e_{31i} r_{si}(x) \frac{\partial^3 w}{\partial x^2\,\partial t} \mathrm{d}x, \quad i = 1, 2, \ldots, N_s, \tag{10b}$$

which have the similar form as those of the straight sensor layer [30].

2.2. ACTUATOR EQUATION

From the constitutive equation of the piezoelectric materials, the stress in directions 1 and 3 induced by the jth actuator fiber can be written as

$$\sigma_{aj1} = -e_{31}E_3, \qquad \sigma_{aj3} = -e_{33}E_3, \qquad j = 1, \ldots, N_a, \tag{11}$$

where σ_1, σ_3 are the stresses in 1 and 3 directions, respectively, E_3 is the electric field along the polling direction (3-axis), N_a is the number of piezoelectric actuator fibers. The stresses induced by the curved actuator fibers in equation (11) can be transformed into the

x direction

$$\sigma_{axj} = -\, e_{31}E_3\cos^2\alpha - e_{33}E_3\sin^2\alpha, \quad j = 1, 2, \dots, N_a, \tag{12}$$

where α is the angle between the tangent of the fiber and the x-axis of the composite beam. The moment resultant can be obtained from

$$M(x) = \iint_S \sigma z \,\mathrm{d}z\,\mathrm{d}y + \sum_{j=1}^{N_a} \iint_{S_{aj}} \sigma_{axj} z\,\mathrm{d}z\,\mathrm{d}y, \tag{13}$$

where S and S_{aj} are the cross-sectional areas of the composite beam and the jth actuator fiber.

When the viscoelastic damping being taken into account in equation (3), substituting equations (3) and (12) into equation (13), gives

$$M(x) = -\, YJ(x)\frac{\partial^2 w}{\partial x^2} - C(x)\frac{\partial^3 w}{\partial x^2\,\partial t} - \sum_{j=1}^{N_a} b_{aj}(e_{31j}\cos^2\alpha_j + e_{33j}\sin^2\alpha_j) r_{aj} V_j, \tag{14}$$

where b_{aj} is the width of the jth actuator fibers, $V_j(x, t)$ the voltage applied on the actuator fiber, $r_{aj} = (z_{1j} + z_{2j})/2$ the z co-ordinate of mid-plane (shape function) of the actuator fiber, and the effective bending stiffness $YJ(x)$ and the effective damping coefficient $C(x)$ of the composite beam are given by

$$\begin{aligned} YJ(x) &= \iint_S Y(x, y, z) z^2\,\mathrm{d}y\,\mathrm{d}z, \\ C(x) &= \iint_S Y(x, y, z)\mu(x, y, z) z^2\,\mathrm{d}y\,\mathrm{d}z, \end{aligned} \tag{15}$$

in which $\mu(x, y, z)$ is the Kelvin–Voigt viscoelastic damping coefficient of the composite beam.

The equilibrium equation for the composite beam can be derived as

$$\rho A(x)\frac{\partial^2 w}{\partial t^2}\,\mathrm{d}x = \frac{\partial^2 M(x)}{\partial x^2}\,\mathrm{d}x + F(x, t)\,\mathrm{d}x, \tag{16}$$

where $\rho A(x)$ is the effective mass density per unit length of the composite beam, and $F(x, t)$ is the distributed transverse loading. Inserting equation (14) into equation (16), yields

$$\begin{aligned} &\rho A \frac{\partial^2 w}{\partial t^2}\,\mathrm{d}x + \frac{\partial^2}{\partial x^2}\left(C\frac{\partial^3 w}{\partial x^2\,\partial t}\right)\mathrm{d}x + \frac{\partial^2}{\partial x^2}\left(YJ\frac{\partial^2 w}{\partial x^2}\right)\mathrm{d}x \\ &= F(x, t)\,\mathrm{d}x - \frac{\partial^2}{\partial x^2}\left[\sum_{j=1}^{N_a} b_{aj} r_{aj}(e_{31j}\cos^2\alpha_j + \mathrm{e}_{33j}\sin^2\alpha_j) V_j\,\mathrm{d}s_j\right]. \end{aligned} \tag{17}$$

Note that $\mathrm{d}x$ is replaced by the infinitesimal arc length $\mathrm{d}s_j$ for each actuator fiber in equation (17) because of its curvature.

Assume that the path occupied by the mid-plane of the jth actuator, $z(x) = r_{aj}(x)$, is smooth, then equation (17) becomes

$$\rho A \frac{\partial^2 w}{\partial t^2} + \frac{\partial^2}{\partial x^2}\left(C \frac{\partial^3 w}{\partial x^2 \partial t}\right) + \frac{\partial^2}{\partial x^2}\left(YJ \frac{\partial^2 w}{\partial x^2}\right)$$

$$= F(x,t) - \frac{\partial^2}{\partial x^2}\left[\sum_{j=1}^{N_a} b_{aj} r_{aj}[e_{31j} + e_{33j} r'^2_{aj}(x)] \frac{V_j(x,t)}{\sqrt{1 + r'^2_{aj}}}\right]. \tag{18}$$

Equation (18) is the actuator equation of the piezoelectric fiber reinforced composite beam and gives the relationship between the transverse vibration and the voltages applied on the actuator fibers.

Assume that the effective damping coefficient $C(x)$ in equation (15) can be estimated by

$$C(x) = \iint_S Y(x,z)\mu(x,z) z^2 \,\mathrm{d}y\,\mathrm{d}z \approx \mu_e \iint_S Y(x,z) z^2 \,\mathrm{d}z = \mu_e YJ(x), \tag{19}$$

where μ_e is an equivalent damping constant. In this case, equation (18) becomes

$$\rho A \frac{\partial^2 w}{\partial t^2} + \mu_e \frac{\partial^2}{\partial x^2}\left(YJ \frac{\partial^3 w}{\partial x^2 \partial t}\right) + \frac{\partial^2}{\partial x^2}\left(YJ \frac{\partial^2 w}{\partial x^2}\right)$$

$$= F(x,t)\,\mathrm{d}x - \frac{\partial^2}{\partial x^2}\left[\sum_{j=1}^{N_a} b_{aj} r_{aj}[e_{31j} + e_{33j} r'^2_{aj}(x)] \frac{V_j(x,t)}{\sqrt{1 + r'^2_{aj}}}\right]. \tag{20}$$

Furthermore, when the curvatures of the actuator fibers are very small, i.e., $r'^2_{aj}(x) \approx 0$, equation (20) can be simplified as

$$\rho A \frac{\partial^2 w}{\partial t^2} + \mu_e \frac{\partial^2}{\partial x^2}\left(YJ \frac{\partial^3 w}{\partial x^2 \partial t}\right) + \frac{\partial^2}{\partial x^2}\left(YJ \frac{\partial^2 w}{\partial x^2}\right) = F(x,t) - \frac{\partial^2}{\partial x^2}\left[\sum_{j=1}^{N_a} b_{aj} e_{31j} r_{aj}(x) V_j(x,t)\right]. \tag{21}$$

Sensor equations (8), (9) or (10), (11) and the actuator equations (18), (20) or (21) derived in this section are the basic equations for active control of the composite beams. In the following sections, the modal sensor and modal actuator as well as the modal control will be discussed based on the simplified sensor and actuator equations.

3. METHOD FOR MODAL SENSOR FIBER DESIGN

Modal sensors can be used to sense the information of the designated modes. Based on the orthogonality of the modes, the modal sensors can be realized by using the piezoelectric sensor fibers.

The transverse displacement $w(x,t)$ of the composite beam can be expressed as a linear superposition of the modes of the beam

$$w(x,t) = \sum_{k=1}^{\infty} W_k(x)\eta_k(t), \tag{22}$$

where $W_k(x)$ is the normal modal function and $\eta_k(t)$ the modal co-ordinate of the composite beam. Substituting equation (22) into the sensor equation (8), we have

$$q_i(t) = -\sum_{k=1}^{\infty} \eta_k(t) \int_0^l p_{si}(x) \frac{d^2 W_k(x)}{dx^2}, \quad i = 1, 2, \ldots, N_s, \tag{23}$$

where

$$p_{si}(x) = b_{si}(x) r_{si}(x) [e_{31i} + e_{33i} r_{si}'^2(x)] / \sqrt{1 + r_{si}'^2} \tag{24}$$

can be called the property function of the ith sensor fiber, and is related to its width, piezoelectric parameter and its shape function. The modal sensors can be designed by properly choosing the property functions of the piezoelectric sensor fibers.

In order to create the modal sensors, the property function of the ith sensor fiber is chosen as

$$p_{si}(x) = c_{si} YJ(x) \frac{d^2 W_i(x)}{dx^2}, \tag{25}$$

where c_{si} is a positive constant. Substituting equation (25) into equation (23) and employing the orthogonality of the modes (for simple homogeneous boundary conditions), the following modal sensor equation can be obtained:

$$q_i(t) = -c_{si} \omega_i^2 \eta_i(t), \tag{26}$$

where ω_i is the ith natural frequency of the composite beam. Consequently, the output current of the modal sensor becomes

$$I_i(t) = -c_{si} \omega_i^2 \dot{\eta}_i(t), \tag{27}$$

where the overdot stands for the first derivative with respect to time t. Equations (26) and (27) show that the output charge (current) of the sensor fiber is proportional to the designated modal co-ordinate (velocity). In other words, the sensor fiber becomes a modal sensor that can measure the designated modal co-ordinate. Therefore, the N_s sensor fibers can be designed to sense N_s modal co-ordinates and modal velocities independently.

It can be seen from equation (24) that there are several methods to realize the modal sensors. The property function can be made to satisfy equation (25) by modulating one of the width, piezoelectric stress parameter and co-ordinate of sensor fiber's neutral plane, or by modulating all the three properties simultaneously.

As a special case, it is assumed that the fibers are straight and piezoelectric parameters of the sensor fibers are constants, and only the width is allowed to be adjusted to create the modal sensor. In this case, the widths of the modal sensors are determined by

$$b_{si}(x) = \frac{c_{si}}{r_{si} e_{31i}} YJ(x) \frac{d^2 W_i(x)}{dx^2}, \quad i = 1, 2, \ldots, N_s, \tag{28}$$

Equation (28) can be used to shape the electrodes of the piezoelectric sensor fibers. Such an idea of designing the modal sensor/actuator, proposed by Lee and Moon [25], can be easily realized for the piezoelectric sensor layer. However, this method is not practical for fibers because its cross-section is sufficiently small compared to its length.

Here we present a new method to design modal sensors by modulating the shape functions of the sensor fibers without changing their width and piezoelectric parameters. In

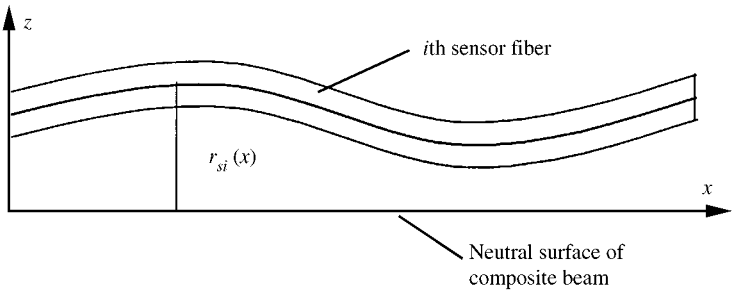

Figure 3. Modal sensor designed by modulating fiber's shape.

this case, the shape function of the ith sensor fiber can be obtained from equations (24) and (25) as

$$r_{si}(x)[e_{31i} + e_{33i}r_{si}'^2(x)]/\sqrt{1 + r_{si}'^2} = \frac{c_{si}}{b_{si}}\, YJ(x)\,\frac{\mathrm{d}^2 W_i(x)}{\mathrm{d}x^2}, \quad i = 1, 2, \ldots, N_s. \tag{29}$$

The shape of the modal sensor fiber can be determined by solving the differential equation with certain boundary conditions. When the curvatures of the sensor fiber is small, the solution of the differential equation (29) can be approximately given by

$$r_{si}(x) = \frac{c_{si}}{b_{si}e_{31i}}\, YJ(x)\,\frac{\mathrm{d}^2 W_i(x)}{\mathrm{d}x^2}, \quad i = 1, 2, \ldots, N_s, \tag{30}$$

which determines the shapes of the sensor fibers, as shown in Figure 3. The constants c_{si} can be used to adjust the shape of the sensor fibers so that the fibers can be accommodated in the beam.

4. METHOD FOR MODAL ACTUATOR FIBER DESIGN

To design the modal actuators, substituting equation (22) into actuator equation (20), and employing the mode orthogonality, the modal equations of motion of the composite beam can be derived as

$$\ddot{\eta}_k(t) + \mu_e\omega_k^2\dot{\eta}(t) + \omega_k^2\eta_k(t) = \int_0^l F(x,t)\,W_k(x)\,\mathrm{d}x - \sum_{j=1}^{N_a}\int_0^l \frac{\partial^2}{\partial x^2}\,[p_{aj}(x)\,V_j(x,t)]\,W_k(x)\,\mathrm{d}x,$$

$$k = 1, 2, \ldots, \tag{31}$$

where

$$p_{aj}(x) = b_{aj}(x)r_{aj}(x)[e_{31j} + e_{33j}r_{aj}'(x)]/\sqrt{1 + r_{aj}'^2}, \quad j = 1, 2, \ldots, N_a, \tag{32}$$

are the property functions of the actuator fibers.

If choosing

$$p_{aj}(x)\,V_j(x,t) = \phi_j(t)\,YJ(x)\,\frac{\mathrm{d}^2 W_j(x)}{\mathrm{d}x^2}, \quad j = 1, 2, \ldots, N_a, \tag{33}$$

in equation (31), the modal equations of the beam will become

$$\ddot{\eta}_k(t) + \mu_e\omega_k^2\dot{\eta}_k(t) + \omega_k^2\eta_k(t) = \begin{cases} f_k(t) - \omega_k^2\varphi_k(t), & k = 1, 2, \ldots, N_a, \\ f_k(t), & k = N_a + 1, \ldots, \end{cases} \tag{34}$$

where $f_k(t) = \int_0^l F(x, t) W_k(x)\,\mathrm{d}x$ is the modal forces contributed by the external load, and $\varphi_k(t)$ the modal force induced by the actuator fiber.

It can be seen from equation (34) that each actuator fiber can be made to excite the designated mode without affecting the other modes by adjusting its property function and the voltage distribution.

There are two categories to design the modal actuators, namely, by modulating the voltage distribution and properties of the actuators respectively. Based on modulating the voltage distribution on the actuator layer, the modal sensors were created for smart beams and plate [29, 30].

When designing the modal actuators by modulating the properties of the actuator fibers, the voltage distribution on the actuator layer or fiber are usually assumed to be uniform, i.e., the voltage on each actuator fiber is only a function of time. In this case, $V_j(x, t) = V_j(t)$, and choosing

$$p_{aj}(x) = c_{aj}\, YJ(x)\frac{\mathrm{d}^2 W_j(x)}{\mathrm{d}x^2}, \quad j = 1, 2, \ldots, N_a, \tag{35}$$

where c_{aj} are also positive constants, the modal actuator equations become

$$\ddot{\eta}_k(t) + \mu_e\omega_k^2\dot{\eta}_k(t) + \omega_k^2\eta_k(t) = \begin{cases} f_k(t) - c_{ak}\omega_k^2 V_k(t), & k = 1, 2, \ldots, N_a, \\ f_k(t), & k = N_a + 1, \ldots. \end{cases} \tag{36}$$

Equation (36) indicates more clearly that each actuator fiber can only actuate one mode when its property function satisfies equation (35). Like the modal sensors design, there are several ways to create the modal actuator by varying one or all of the widths, the piezoelectric parameters, as well as the shapes of the mid-surfaces of the actuator fibers.

Designing the modal actuator by modulating the electrode patterns of the actuator [25] is not practical for fibers. Here, for the fine piezoelectric actuator fibers, we give a new method to design the modal actuators by shaping the mid-surfaces of the actuator fibers.

The shape function of the jth actuator fiber can be obtained by solving the following differential equations:

$$r_{aj}(x)[e_{31j} + e_{33j}r_{aj}'^2(x)]/\sqrt{1 + r_{aj}'^2} = \frac{c_{aj}}{b_{aj}}\, YJ(x)\frac{\mathrm{d}^2 W_j(x)}{\mathrm{d}x^2}, \quad j = 1, 2, \ldots, N_a. \tag{37}$$

Note that equation (37) has the same form of equation (29), which means that a modal sensor fiber can also be used as a modal actuator. When the curvatures of the actuator fibers are small, the approximate solution of equation (37) is given by

$$r_{aj}(x) = \frac{c_{aj}}{b_{aj}e_{31j}}\, YJ(x)\frac{\mathrm{d}^2 W_j(x)}{\mathrm{d}x^2}, \quad j = 1, 2, \ldots, N_a. \tag{38}$$

The shape of each actuator fiber with uniform thickness can be determined by equation (38), just the same as the modal sensor design as shown in Figure 3. The constants c_{aj} in equation

(38) can be used to control the shape of each actuator fiber so that it is suitable to be embedded in the host beam. In this way, the N_a actuator fibers can be designed to N_a modal actuators, which can excite N_a modes independently.

5. INDEPENDENT MODAL SPACE CONTROL OF COMPOSITE BEAM

Independent modal control can be realized using the modal sensors and modal actuators created in the previous sections, i.e., several modes of the beam can be controlled independently with the modal sensors and actuators.

For the free vibration case, the modal equations of motion are given by

$$\ddot{\eta}_k(t) + \mu_e \omega_k^2 \dot{\eta}_k(t) + \omega_k^2 \eta_k(t) = \begin{cases} -\, c_{ak}\omega_k^2 V_k(t), & k = 1, 2, \ldots, N, \\ 0, & k = N+1, \ldots, \end{cases} \tag{39}$$

where N is the number of controlled modes and $N \leqslant \min(N_s, N_a)$. To perform the modal control, the control voltage should be designed for each actuator fiber according to some control laws. Here the simply proportional and derivative (PD) controller is employed and the control voltage is designed by

$$V_k(t) = -\, g_{1k}(t) q_k(t) - g_{2k}(t) I_k(t), \quad k = 1, 2, \ldots, N, \tag{40}$$

where $g_{1k}(t)$ and $g_{2k}(t)$ are non-negative control gains, which may be designed as time-dependent.

Inserting the modal sensor equations (26) and (27) into equation (40), gives

$$V_k(t) = g_{1k}(t) c_{sk} \omega_k^2 \eta_k(t) + g_{2k}(t) c_{sk} \omega_k^2 \dot{\eta}_k(t), \quad k = 1, 2, \ldots, N. \tag{41}$$

Substituting the feedback control voltages from equation (41) into equation (39), the closed-loop modal equations of motion for the controlled modes are obtained as

$$\ddot{\eta}_k(t) + [\mu_e \omega_k^2 + g_{2k}(t) c_{sk} c_{ak} \omega_k^4] \dot{\eta}_k(t) + [g_{1k}(t) c_{sk} c_{ak} \omega_k^4 + \omega_k^2] \eta_k(t) = 0, \quad k = 1, 2, \ldots, N, \tag{42}$$

and the uncontrolled mode (residual modes) are not affected by the active control. Equation (42) indicated that the active damping is achieved for each controlled mode due to the modal control. For the case that the control gains are constants, the active damping ratios can be calculated as

$$\zeta_k = \frac{g_{2k} c_{sk} c_{ak} \omega_k^3}{2\sqrt{1 + g_{1k} c_{sk} c_{ak} \omega_k^2}}, \quad k = 1, 2, \ldots, N, \tag{43}$$

which will decay the controlled modes significantly by properly choosing the control gains. In addition, the feedback of the modal co-ordinates increases the frequencies of the controlled modes of the beam, which will lead to suppression of the vibration amplitude. The displacements of the composite beam can be obtained by substituting the modal co-ordinates from equation (42) into equation (22).

6. AN ILLUSTRATIVE EXAMPLE

As an illustrative example, consider a cantilevered composite beam in which four sensor fibers and four actuator fibers are embedded. All the piezoelectric fibers are made of the

TABLE 1

Material and dimensional parameters

Item	Host beam (glass/polyester)	Piezofibers (PZT-5A)
Mass density (kg/m^3)	1930	7600
Young's modulus (GPa)	38	53
Piezoconstant d_{31} (m/V)	—	370×10^{-12}
Piezoconstant d_{33} (m/V)	—	392×10^{-12}
Thickness (m)	0·003	0·0004
Length (m)	0·5	
Width (m)	0·03	0·0005

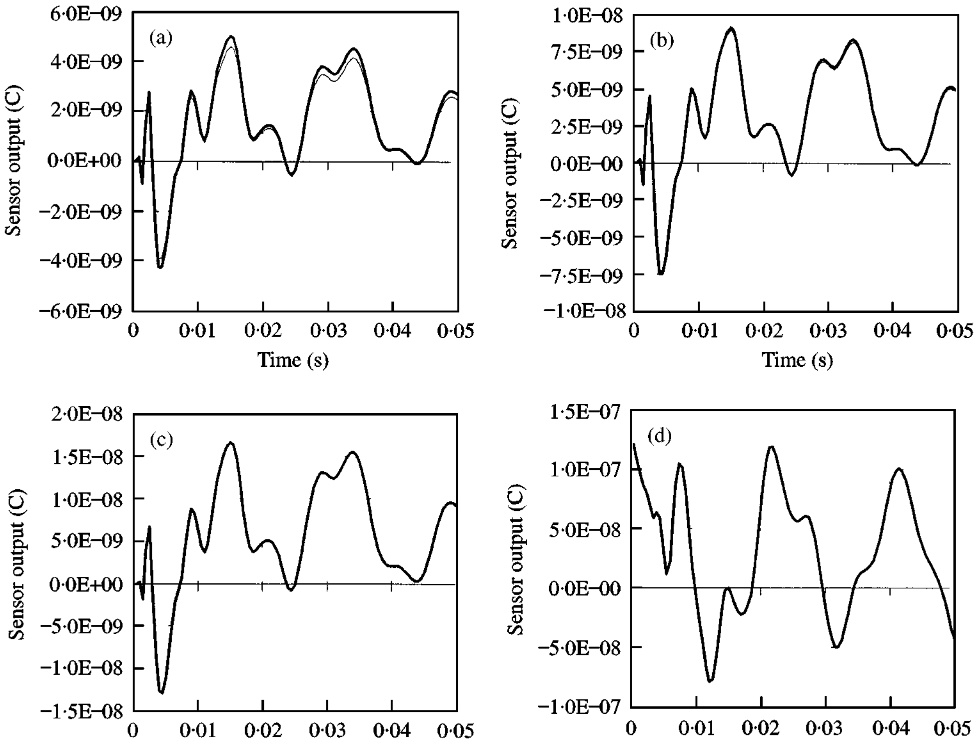

Figure 4. Output charges of sensor fibers with curvature $r_s(x) = -(h_b/2) + (h_b/2)\cos(\pi x/2l_s)$: ——, approximate results; ——, exact results. (a) $ls = 5$ mm ($a/ls = 3/10$); (b) $ls = 1$ cm ($a/ls = 3/20$); (c) $ls = 2$ cm ($a/ls = 3/40$); (d) $ls = 50$ cm ($a/ls = 3/1000$).

same lead zirconate titanate (PZT) material and have the same width and thickness. The material properties and dimensions of the composite beam are listed in Table 1. In this example, the effects of the piezoelectric fibers on the mass density and the bending stiffness are neglected because of their small volume portions. In the following discussion, the free vibration of the composite beam is caused by an impulse of 8×10^{-5} N s acting on it free end. In this simulation, the equivalent viscoelastic-damping coefficient μ_e is assumed as

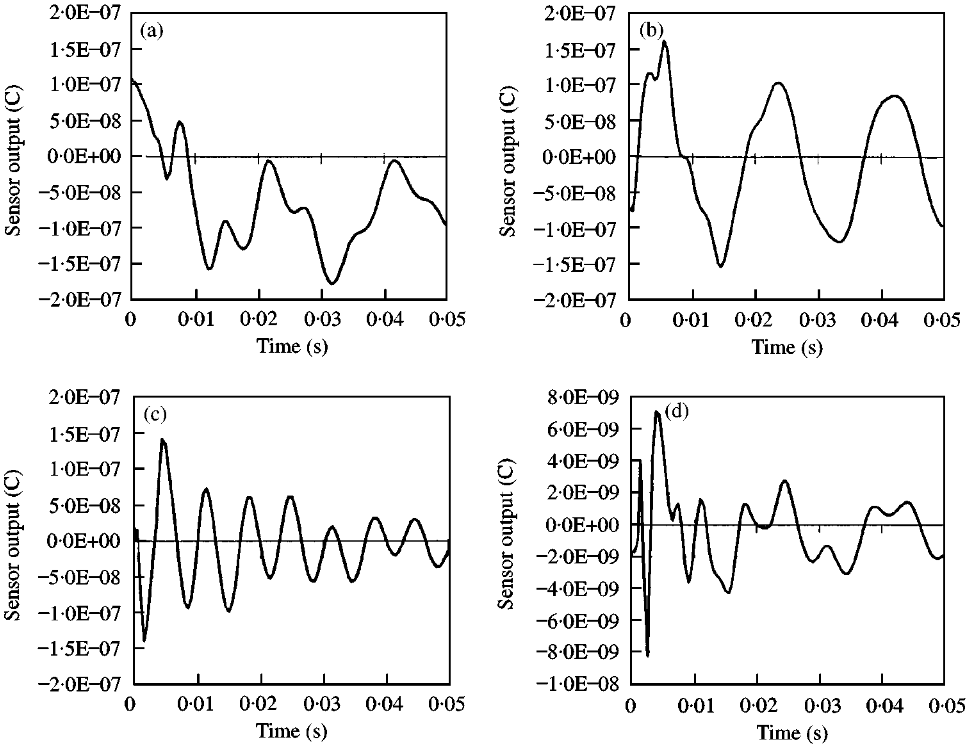

Figure 5. Output charges of sensor fibers with curvature $r_s(x) = (3h_b/4)\cos(k\pi s/2l_s)$: ——, approximate results; ——, exact results. (a) $k = 1$; (b) $k = 2$; (c) $k = 3$; (d) $k = 10$.

0·008%. The first several natural frequencies are 8·60, 53·91, 150·93, 295·77 and 488·93 Hz respectively.

First, comparison of the output charges of the sensor fibers between exact and approximate formula will be made to examine the effect of the curvature of the fibers on its output. To this end, consider a set of sensor fibers integrated in the composite beam and their shape functions have the form $r_s(x) = r_{s0} + a\cos\pi x/2l_s$. Taking $r_{s0} = -h_b/2$, and $a = h_b/2$, the charges generated by the sensor fibers with different $l_s(l_s = 0{\cdot}005, 0{\cdot}01, 0{\cdot}02, 0{\cdot}50$ m) are shown in Figure 4, in which both the exact results from equation (8) and approximate ones from equation (10) are given. It can be seen that the error of the approximate formula in equation (10) is remarkable when the l_s is very short (i.e., the slope of fiber is large). However, as the length of the sensor fiber increases, the error decreases so rapidly that it can be neglected. So the approximate formula can be used and can give a good estimation if all the fibers have a small number of repeating waves.

Next, we check the output charge of the curved sensor fibers with different shapes. The shape function $r_s(x)$ is chosen as $r_s(x) = (3h_b/8)\cos(k\pi x/2l)$. When $k = 1, 2, 3, 10$, the output charges of the sensor fibers calculated both from the exact and approximate formula are depicted in Figure 5. In this case, the differences between the results obtained by equations (8) and (10) cannot be displayed even for the case that the wave number is 20. It shows that the simplified formula equation (10) can give satisfactory results for a slender composite beam. Therefore, the simplified equation (30) can be used to determine the shapes of the modal sensors even for the relatively high order modes. It is also seen that a specifically shaped fiber sensor tends to be more sensitive to the vibration mode having the similar

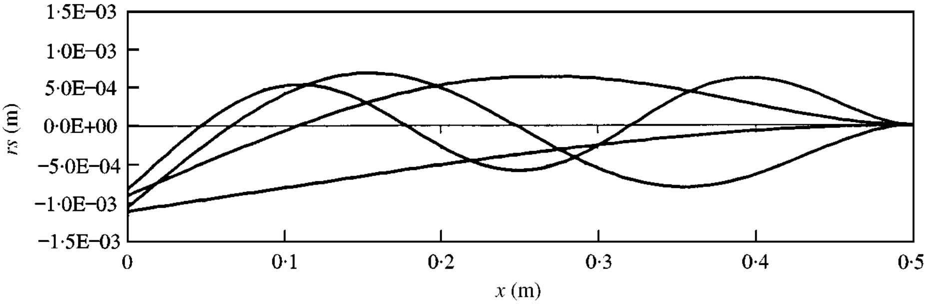

Figure 6. The curvature shapes of the four modal sensor fibers.

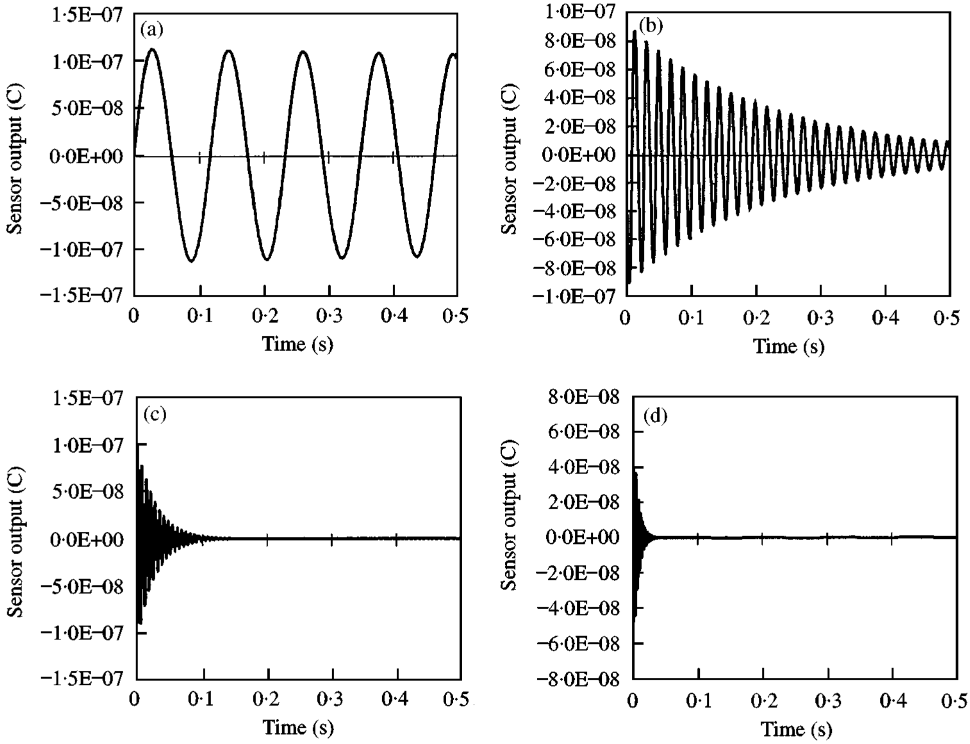

Figure 7. The outputs of the four modal sensor fibers: (a) modal sensor fiber 1; (b) modal sensor fiber 2; (c) modal sensor fiber 3; (d) modal sensor fiber 4.

shape. For example, the fibers with curvatures $a\cos(2\pi x/2l)$ and $a\cos(3\pi x/2l)$ are more sensitive to the second and the third modes of the beam respectively. In general, the fiber with higher wave number k is sensitive to higher modes of the composite beam. Therefore, by properly chosing the shape of the sensor fiber, the modal sensor can be created which can only sense the given mode.

To design the modal sensor, the curvature shapes of the four sensor fibers should be determined by solving equation (30). The constants $c_s(c_a)$ for both the sensor and actuator fibers are chosen as $4{\cdot}6\times10^{-4}b_se_{31}$, $6\times10^{-5}b_se_{31}$, $2{\cdot}5\times10^{-5}b_se_{31}$, $1\times10^{-5}b_se_{31}$,

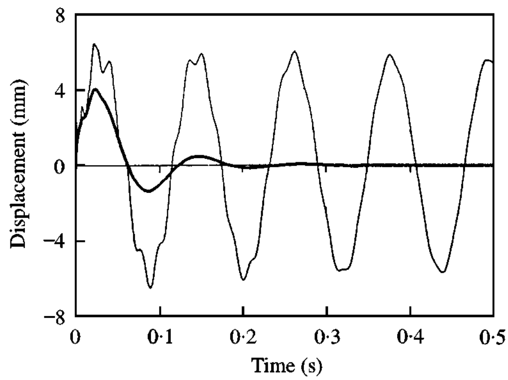

Figure 8. Displacement of the free end of the beam; ——, uncontrolled; ——, controlled.

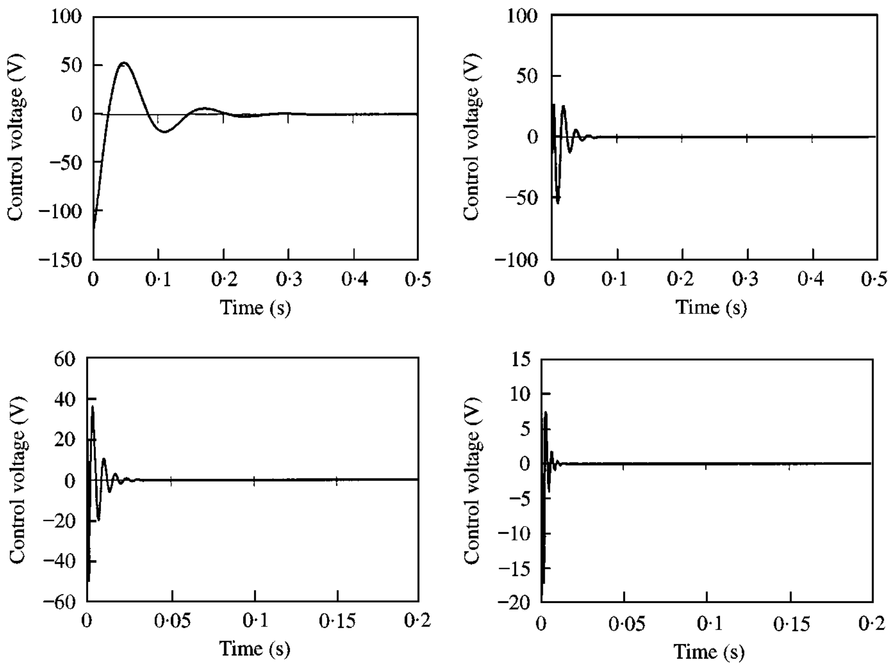

Figure 9. Control voltages on the four modal actuator fibers: (a) actuator fiber 1; (b) actuator fiber 2; (c) actuator fiber 3; (d) actuator fiber 4.

respectively, in order to make the modal sensor/actuator fibers suitable to be embedded in the beam. In this case, the shapes of the four modal sensor fibers are drawn in Figure 6 and their output charges are given in Figure 7. Following the same procedures, the four modal actuator fibers can be designed. In fact, the four modal sensor fibers can also be used as the modal actuators due to the reciprocal relationship between the sensor and actuator fibers. The modal sensor/actuator fibers are embedded into the host composite beam, the modal control can be performed.

The high order modes of the beam have been damped out remarkably by the natural viscoelastic damping, as shown in Figure 7. Therefore, only the several low order modes should be controlled. Here the first four modes are selected as the controlled modes. When

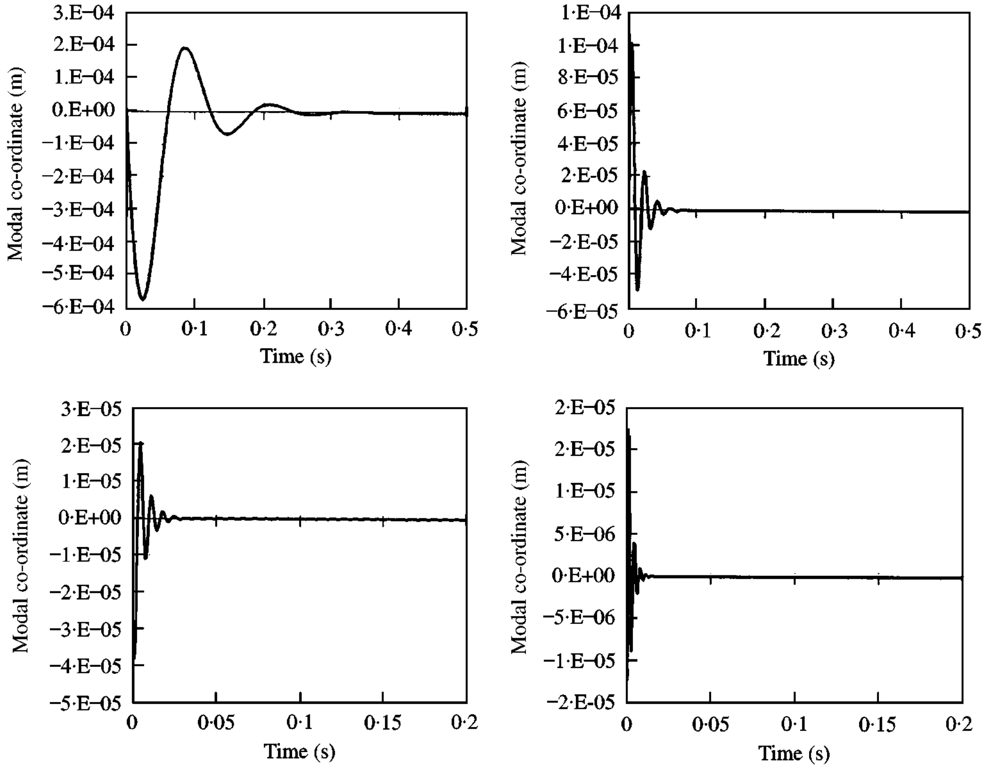

Figure 10. Modal co-ordinates for controlled modes.

the control gains in equation (40) are taken as $g_{11} = 5000$, $g_{21} = 200\,000$; $g_{12} = 4000$, $g_{22} = 32\,000$; $g_{13} = 3000$, $g_{23} = 6000$; $g_{14} = 2000$, $g_{24} = 2000$, the displacement at the free end of the controlled beam is shown in Figure 8. The four controlled modes and the voltages applied on the modal actuators are also given in Figures 9 and 10 respectively. The control results show that the vibration of the composite beam is controlled effectively within a short time because all the control energy is fully used to control the low modes.

7. CONCLUSIONS

In this paper, the vibration control of a composite beam with curved piezoelectric fibers is studied. The sensor equations and actuator equations of the curved fibers are derived by employing line integrals. Moreover, a new method to design modal sensors and modal actuator is given by means of shaping the curvatures of the piezoelectric fibers. Unlike the straight fibers, the sensing and actuating of the curved fibers are affected by their piezoelectric constants e_{31} and e_{33} as well as their curvatures. If the curvatures of the fibers are small, their effect can be neglected. However, while designing the high order modal sensor or modal actuator, the curvatures of the fibers should be considered in order to avoid the observation and control spillover. With the modal sensors and modal actuators designed using the curved piezoelectric fibers, the independent modal space control can be performed and good control results have been achieved.

ACKNOWLEDGMENT

The author are grateful to the support rendered by the Australian Research Council and by the National Science Foundation of China (Grant No. 19802016).

REFERENCES

1. T. BAILEY and J. E. HUBBARD 1985 *Journal of Guidance, Control and Dynamics*, **8**, 650–611. Distributed piezoelectric-polymer active vibration control of a cantilever beam.
2. E. F. CRAWLEY and J. DE LUIS 1987 *American Institute of Aeronautics and Astronautics Journal* **25**, 1373–1385. Use of piezoelectric actuators as elements of intelligent structures.
3. S. IM and S. N. ATLURI 1989 *American Institute of Aeronautics and Astronautics Journal* **27**, 1801–1807. Effects of piezo actuator on a finitely-deformed beam subjected to general loading.
4. E. F. CRAWLEY and E. H. ANDERSON 1990 *Journal of Intelligent Material Systems and Structures* **1**, 4–25. Detailed models of piezoelectric isotropic and anisotropic plates.
5. B. T. WANG and C. A. ROGERS 1991 *Journal of Intelligent Material Systems and Structures* **2**, 38–58. Modeling of finite-length spatially-distributed induced strain actuators for laminated beams and plates.
6. E. K. DIMITRIADIS, C. R. FULLER and C. A. ROGERS 1991 *Journal of Vibration and Acoustics* **113**, 100–107. Piezoelectric actuators for distributed vibration excitation of thin plates.
7. H. S. TZOU and M. GADRE 1989 *Journal of Sound and Vibration* **132**, 433–450. Theoretical analysis of a multi-layered thin shell coupled with piezoelectric shell actuators for distributed vibration controls.
8. S. S. RAO and M. SUNAR 1994 *Applied Mechanics Review* **47**, 113–123. Piezoelectricity and its use in disturbance sensing and control of flexible structures: a survey.
9. E. F. CRAWLEY 1994 *American Institute of Aeronautics and Astronautics Journal* **32**, 1689–1699. Intelligent structures for aerospace: a technology overview and assessment.
10. R. G. LOEWY 1997 *Smart Materials and Structures* **6**, R11–R42. Recent developments in smart structures with aeronautical applications.
11. C. CHEE, L. TONG and G. P. STEVEN 1998 *Journal of Intelligent Material Systems and Structures* **9**, 3–19. A review on the modeling of piezoelectric sensors and actuators incorporated in intelligent structures.
12. H.-S. TZOU and C. I. TSENG 1991 *Journal of Dynamic Systems, Measurements and Control* **113**, 494–499. Distributed modal identification and vibration control of continua: theory and application and analysis.
13. C. CHEE, L. TONG and G. P. STEVEN 1999 *Smart materials and Structures* **8**, 417–432. A mixed model for composite beams with piezoelectric actuator sand sensors.
14. K. CHANDRASHEKHARA and A. N. AGARWAL *Journal of Intelligent Material Systems and Structures*, **4**, 496–508. Active vibration control of laminated composite plates using piezoelectric devices.
15. W.-S. HWANG, H. C. PARK and W. HWANG 1993 *Journal of Intelligent Material Systems and Structures* **4**, 317–329. Vibration control of a laminated plate with piezoelectric sensor/actuator: finite element formulation and modal analysis.
16. S. DEVASIA, T. MERESSI and B. PADEN 1993 *Journal of Guidance, Control and Dynamics* **16**, 859–864. Piezoelectric actuator design for vibration suppression: placement and sizing.
17. F. FAKHROO 1993 *SPIE* **2442**, 304–313. Optimal location of piezoelectric actuators for vibration suppression of flexible structures.
18. K. Y. SZE, L. Q. YAO and S. YI 2000 *International Journal for Numerical Methods in Engineering* **48**, 565–582. A hybrid-stress ANA solid-shell element and its generalization for smart structure modelling. Part II: smart structure modelling.
19. W. READER and D. SAUTER 1993 *Proceedings of Damping '93, San Francisco*, GBB 1–18. Piezoelectric composites for use in adaptive damping concepts.
20. W. SHIELDS, J. RO and A. BAZ 1998 *Smart Materials and Structures* **7**, 1–11. Control of sound radiation from a plate into a acoustic cavity using active piezoelectric-damping composites.
21. A. A. BENT, N. W. HAGOOD and J. P. RODGERS 1995 338–349. *Journal of Intelligent Material Systems and Structures* **6**, 338–349. Anisotropic actuation with piezoelectric fiber composites.
22. A. A. BENT and N. W. HAGOOD 1997 *Journal of Intelligent Material Systems and Structures* **8**, 903–919. Piezoelectric fiber composites with interdigitated electrodes.

23. B. Z. JANOS and N. W. HAGOOD 1998 *Proceedings of the six International Conference on New Actuators ACTUATOR*98, Bremen, Germany. Overview of Active Fiber Composites Technologies.
24. L. MEIROVTCH 1990 *Dynamics and Control of Structures*. New York. Wiley-Interscience.
25. C.-K. LEE and F. C. MOON 1990 *Journal of Applied Mechanics* **57**, 434–441. Modal sensors and actuators.
26. C.-K. LEE, W.-W. CHIANG and T. C. O'SULLIVAN 1991 *Journal of Acoustics Society of America* **90**, 374–384. Piezoelectric modal sensor/actuator pairs of critical active damping vibration control.
27. H. S. TZOU, J. P. ZHONG and J. J. HOLLKAMP 1994 *Journal of Sound and Vibration* **174**, 363–378. Spatially distributed orthogonal piezoelectric shell actuators: theory and applications.
28. Y. GU, R. L. CLARK and C. R. FULLER 1994 *Journal of Vibration and Acoustics* **116**, 303–308. Experiments on active control of plate vibration using piezoelectric actuators and polyvinylidene fluoride (PVDF) modal sensors.
29. S. E. MILLER, Y. OSHMAN and H. AVRAMORICH 1996 *American Institute of Aeronautics and Astronautics Journal* **34**, 1868–1875. Modal control of piezolaminated anisotropic rectangular plates. Part 1: modal transducer theory.
30. D. C. SUN, D. J. WANG and Z. L. XU 1997 *American Institute of Aeronautics and Astronautics Journal* **35**, 583–584. Distributed piezoelectric segment method for vibration control of smart beams.
31. D. C. SUN, D. J. WANG and Z. L. XU 1999 *American Institute of Aeronautics and Astronautics Journal* **37**, 1459–1463. Distributed piezoelectric element method for vibration control of smart plates.
32. D. C. SUN and L. TONG *International Journal of Solids and Structures*, in press. Modal control of smart shells by optimized discretely distributed piezoelectric transducers.